Available online at www.sciencedirect.com

jmr&t Journal of Materials Research and Technology

journal homepage: www.elsevier.com/locate/jmrt

Original Article

Production of low-cost adsorbent with small particle size from calcium carbonate rich residue carbonatation cake and their high performance phosphate adsorption applications

Hasan Arslanoğlu [1]

Kırşehir Ahi Evran University, Faculty of Engineering and Architecture, Department of Chemical and Process Engineering, 40100 Kırşehir, Turkey

ARTICLE INFO

Article history:
Received 2 July 2020
Accepted 14 January 2021
Available online 22 January 2021

Keywords:
Phosphorus removal
Adsorption
Residue carbonatisation cake
Calcine carbonatisation cake

ABSTRACT

This study investigated phosphorus removal from aqueous solutions using carbonatisation cake, which is a sugar residue containing a significant amount of reactive calcium carbonate. The chemical composition of the carbonatisation cake was determined, and the organic contamination of the carbonatisation cake and calcine in contact with water was determined. In addition, TGA, DTA, XRD, SEM-EDX, BET, FTIR, density, pHzpc and particle size distribution were analyzed for carbonatisation cake, product and post-phosphate removal calcined product. Batch experiments were performed to determine the effect of dose, phosphorus concentration, temperature and contact time on phosphorus removal from aqueous medium. Maximum phosphate adsorption capacity was found to be 65.16 mg g^{-1} at 25 °C, pH of 6 and adsorbent dosage of 1 g L^{-1} for a contact time of 180 min. Adsorption experiments were applied to adsorption isotherms. Kinetic, thermodynamic and mass transfer calculations were calculated. The results show that calcines produced by heating the carbonated cake to 600 °C, which is not cost-effective in sugar production, can be used effectively to remove phosphate from wastewaters.

1. Introduction

Advances in technology not only provide a comfortable life but also cause some important problems, one of which is environmental pollution [1]. The aquatic environment is the environment where most pollutants are transported, and the risk of contamination is highest. The amount of domestic wastes is increasing continuously due to increasing population [2,3]. Domestic wastes contain pollutants that constitute a hazard to surface waters. The most important part of this group of pollutants is phosphorus compounds. Domestic waste waters contain significant amounts of phosphorus due to human wastes and household detergents. Phosphorus has a special significance as it is the key element of the phenomenon known as eutrophication, which is defined as the enrichment of surface waters with nutrients and thus algae. Here, the definition of the key elements is not

E-mail address: hasan.arslanoglu@ahievran.edu.tr.
[1] Fax: +90 386 280 38 01.

https://doi.org/10.1016/j.jmrt.2021.01.054

random because 16 parts of nitrogen, 106 parts of carbon and only 1 part of phosphorus are needed for the formation of algae protoplasm [4–7]. Eutrophication caused by the release of phosphorus into the water bodies can lead to significant problems such as a decrease in the recreational value of surface waters, extinction of fish species, difficulty in water transportation and risk for human health. It is, therefore, necessary to reduce phosphorus concentrations below the permissible limits before industrial or domestic wastes are discharged [8,9]. Water sources with a total phosphorus concentration of 0.02 mg L^{-1}, 0.16 mg L^{-1}, 0.65 mg L^{-1} and >0.65 mg L^{-1} are defined as first-, second- third- and fourth-quality waters, respectively. Some studies have reported that lake waters contain about 0.14 mg L^{-1} of dissolved phosphorus and about 0.40 mg L^{-1} of ortho phosphate phosphorus [3,8,9].

Phosphates can be removed from water using biological and chemical processes or a combination of them. These conventional techniques are, however, insufficient for a good treatment. For example, biological treatment removes 20–40% of phosphates. The elimination of activated sludge is also another important problem in such processes. Chemical treatments, on the other hand, require expensive chemicals and cause chemicals to be passed to secondary pollutants [8,9]. The insufficiency of conventional treatment methods and economic reasons have led to continuous research on phosphate treatment and some modern treatment techniques such as adsorption, reverse osmosis and electrodialysis have been developed. Of these methods, adsorption is the most effective and therefore has been intensively investigated. Altundoğan et al. [8] reported that an adsorption system with activated alumina reduced the phosphorus content below 0.5 mg L^{-1} in the waste water in a wastewater treatment plant in Berlin [8,9]. Iron, aluminum and lime have been widely used as adsorbents for the removal of phosphates from wastewater. The phosphate adsorption capacities of alumina, aluminum hydroxide, iron (III) hydroxide, geotite and hematite have been investigated in detail. The adsorption of phosphate with iron- and aluminum-based industrial wastes such as red mud, pyrite ash, ferrochrome slag and thermal power plant fly ash have also been investigated. Results have shown that iron and aluminum-based adsorbents have high affinity for phosphate [10–16]. Most adsorbents are manufactured and expensive, and therefore, their use for phosphate removal is not cost-effective. However, adsorption capacities of these residues are generally low and require chemically activating processes [17–20].

Carbonatisation cakes containing calcium carbonate and colloidal substances of organic origin composed of calcium carbonate are formed at the end of the sherbet treatment process. These residues with high organic matter pollution load are treated in some sugar factories. Various methods have been developed for the reclamation of lime, use in cement production and regeneration of acidic soils for the evaluation of these wastes [21–23]. Since carbonate cake contains a large amount of calcium carbonate, it can be used for phosphate adsorption. Carbonatisation cake is formed in a very small particle size as a result of the reaction of dissolved calcium hydroxide with carbon dioxide in carbonatisation, and it may be an effective adsorbent due to its formation in a relatively basic medium. However, carbonatisation cake and colloidal organic substances from the beet itself can increase the organic pollution of the water environment during sorption. In that situation, organic organisms can be heated at temperatures not too high for pyrolysis to prevent carbonatisation cake formation and thus secondary pollution.

This study investigated whether Carbonatisation cake can be used to remove phosphate ions from aqueous media. Batch systematic experiments were performed to investigate the obtained calcines, and the adsorption of phosphorus from the samples containing hypothetical wastewater containing phosphate was investigated.

Table 1 – Chemical composition of carbonatisation cake used in experiments.

Component	Compound (%)
CaO	49.8
MgO	3.56
K_2O	0.11
Na_2O	0.15
FeO	0.12
Analysis undetectable	2.46
Weight Loss (50–850 °C)	43.8

2. Materials and methods

2.1. Materials

The first carbonatisation cake used in the experiments was supplied from the Elazığ Sugar Factory during the 2016 campaign period. The carbonatisation cake was removed from the outlet of the rotary filter and dried on a nylon tarpaulin in a room atmosphere. It was then milled and sieved. The −200 mesh (<75 μm) fraction was stored in glass-lid jars during the experiments after drying for 2 h in an oven at 80 °C. Table 1 shows the chemical composition of the carbonatisation cake in terms of oxides.

2.2. Preparation of calcination product

Calcined products were prepared just before the experiments. The 25 g carbonatisation cake with a −200 mesh size

Table 2 – Some properties of carbonatisation cake.

Property	Value
Bulk density (g cm^{-3})	0.961
True density (g cm^{-3})	1.837
BET surface area (m^2 g^{-1})	47.6
Langmuir surface area (m^2 g^{-1})	59.3
[a] Pore volume (cm^3 g^{-1})	0.3961
[b] Pore size (Å)	156.38
Particle size [vol. weighted mean, (D [3,4]), μm]	15.75
Particle size [d (0.1), μm]	3.91
Particle size [d (0.5), μm]	12.75
Particle size [d (0.9), μm]	28.63

[a] Total pore volume of pores less than 1262 Å width.
[b] Adsorption average pore width (4 V/A by BET).

Table 3 – Weight losses determined during the calcination of the carbonatisation cake used in the experiments.

Calcination Temperature (°C)	Weight Loss (%)	COD (mg-O_2/L)
200	5.55	62.4
300	7.90	47.6
400	10.12	29.1
500	11.35	11.8
600	13.26	0.09
700	38.76	0.04
800	47.86	0.01

was placed in 100 mL porcelain pots and calcined for 2 h in an open oven (Protherm PLF 110/15). Calcination was performed between 200 and 800 °C. The calcined cakes were cooled in a desiccator and stored in glass cups with tightly closed wells.

2.3. *Adsorption experiment*

Batch adsorption experiments were carried out in 250 mL flasks with plastic lids. Phosphate-containing solutions were prepared from $NaH_2PO_4.2H_2O$ (Sigma Aldrich) salt. The phosphate solutions with the required initial concentrations were prepared by appropriate dilutions from stock solutions at 100 mg-P/1. Then, solutions with specific phosphorus concentrations were moved to flasks to measure their pH using a Mettler Delta 3000 pH meter. Then, appropriate amounts of calcined carbonatisation cake samples weighed ±0.001 g were added to the solutions. The flasks were then tightly sealed and placed in a fixed temperature orbital shaker (Zhecheng, ZHWY-200D) and agitated at 400 rpm. At the end of the time periods, some of the samples from the shaker were filtered through the blue tape filter paper, and the final pH of the mixtures was immediately measured. Phosphorus contents of the filtrates obtained after separation were determined. Then, removal efficiencies and adsorption densities were calculated using the following formulas.

$$\%\ \text{Phosphate Adsorption} = (C_o - C_s) \times \frac{100}{C_o} \quad (1)$$

$$q = \frac{(C_o - C_s) \times V}{m} \quad (2)$$

where C_0 and C are the phosphate concentration (mg-P L^{-1}) at the beginning and end of contact at the solution, respectively; q is the adsorption capacity (mg-P g^{-1}) and m is the adsorbent dose (g L^{-1}).

The effect of pH on phosphate removal was determined by shaking for 1440 min using 50 mg-P L^{-1} 0.5 g L^{-1} -200 mesh calcined carbonatisation cake at 25 °C. The effect of the adsorbent dose on phosphate removal was investigated by adding 0.1–10 g L^{-1} of 200 mesh calcined carbonatisation cake at 50 mg-P L^{-1}, 25 °C and the original pH and by shaking for 1440 min. The effect of calcined carbonatisation cake on phosphate removal time was examined at experiments at different temperatures between 5 and 1440 min using 0.5 g L^{-1} -200 mesh calcined carbonatisation cake at 50 mg-P L^{-1} concentrations at the original pH at 25, 40 and 55 °C. The effect of the initial concentration was examined at 25, 40 and 55 °C, original pH, different concentrations (10-50 mg-P L^{-1}), 0.5 g L^{-1} -200 mesh calcined carbonatisation cake dose for 240 min.

Experiments were carried out in two parallel samples. When the results showed a maximum deviation of 5% from each other, the calculations were made by taking the average of the two parallel experiments. A third experiment was performed in cases with more deviation, and the average of the two experiments that were close to each other were taken into account.

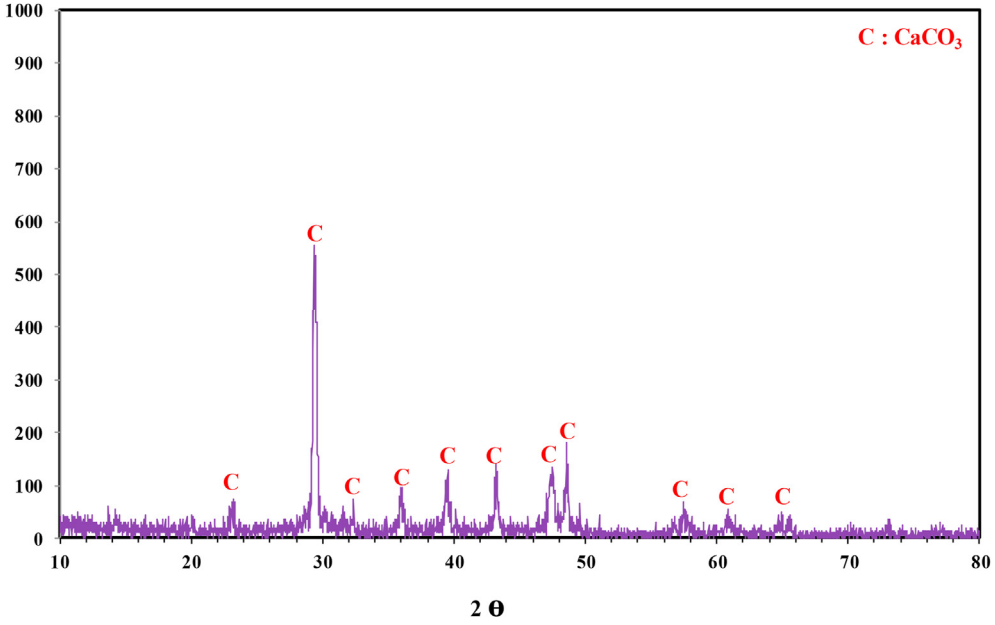

Fig. 1 – X-ray diffractogram of carbonatisation cake.

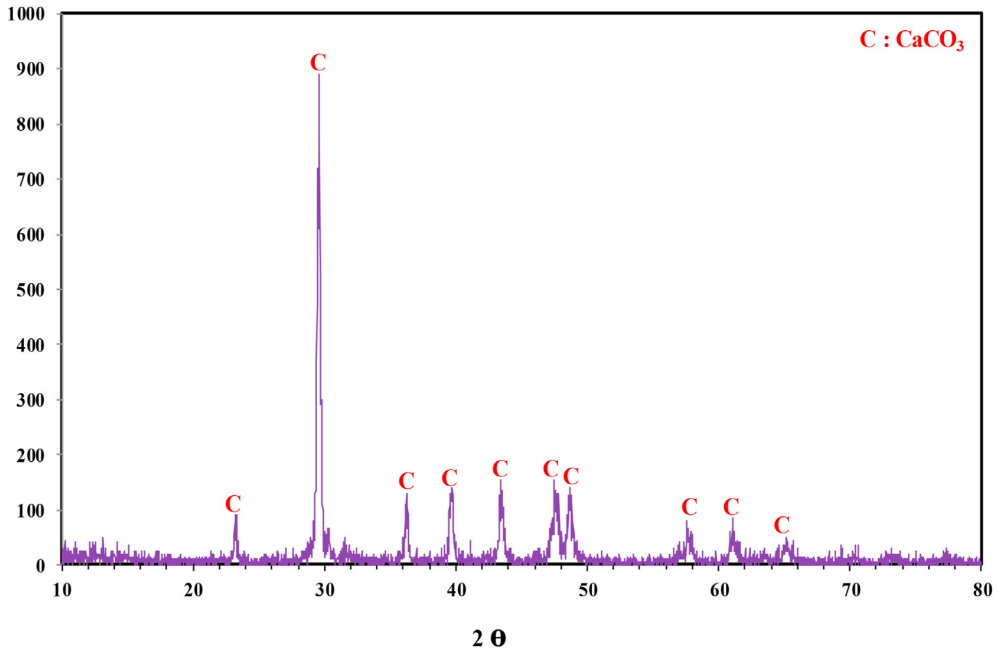

Fig. 2 – X-ray diffractogram of the product obtained by calcining the carbonatisation cake.

2.4. *Instrumentation and measurements*

The characterization of the carbonatisation cake and calcination product was performed using proximate and ultimate analysis, elemental analysis (LECO CHNS 932 Elemental Analyzer), X-ray diffraction (XRD, Rigaku D-max-2200), FT-IR (PerkinElmer Spectrum 100), TGA-DTA (FEI Quanta 250 FEG) and SEM-EDS (FEI Quanta 250 FEG), BET surface area (Micromeritics ASAP 2020), particle size distribution (Malvern Master Sizer 3000), pHzpc (Malvern Nanosize ZS-3600 zetasizer), COD analysis in terms of ASTM D1252 - 06.

2.5. *Elemental analysis*

Ca, Mg, Na, K, Fe analyses were performed on the carbonatisation cake in a ICP-MS (PerkinElmer NexION-2000) device. There are several methods proposed for the spectrophotometric determination of ortho-phosphates. One of them is the ascorbic acid method, which was used in this study. It was originally developed by Altundoğan et al. [9] and is considered to be one of the standard ortho-phosphate determination methods in AWWA, APHA, WPCF [24].

3. Results and discussion

3.1. *Carbonatisation cake*

Table 1 shows the chemical composition of the carbonatisation cake in terms of oxides. Some organic and inorganic acids from the beetroot and soluble salt are not as high as calcium salts during calcination, it can, therefore, be assumed that a very large part of calcium is in the form of calcium carbonate. Considering that cake is formed under the conditions of the first carbonatisation and the pH ranges from 10.8 to 11.2, it can be assumed that only a small portion of calcium is CaO. Table 2 shows the characteristics of the carbonatisation cake.

Table 3 shows the weight losses and COD values of the calcines prepared by heating the carbonate cake for 3 h between 200 and 800 °C. Burning of organics in the carbonatisation cake and calcination of calcium carbonate and some organic calcium salts lead to weight loss. It is noteworthy that the calcine obtained at 200 °C is increasingly darker. The calcine, which is dark black at 600 °C, becomes gradually light color from 700 °C on and is calcined white at 800 °C. It was determined that burning with restricted air in the oven resulted in the carbonization of the organic matter in the cake at low temperatures. Combustion was more efficient at higher temperatures, resulting in the formation of calcium oxide, which was light color [21].

The organic contamination of the carbonatisation cake and its calcined products at various temperatures was determined by contacting the water for 120 min at the doses where the

Table 4 – Comparison of XRD peaks with calcium carbonate values in mindact.org[a].

d distance	2θ angle calculated from Bragg equation[b]	Intensity	Comparison
3.86	22.75	10	√
3.04	29.16	100	√
2.85	30.63	17	√
2.50	34.80	18	√
2.29	39.17	18	√
2.10	41.15	10	√
1.93	44.59	11	√
1.91	47.03	38	√
1.88	48.71	12	√

[a] https://www.mindat.org/min-859.html.
[b] $n\lambda = 2d\sin\theta$ (Bragg equation)[$n = 1$; $\lambda = 1.5418$ (Cu Kα)].

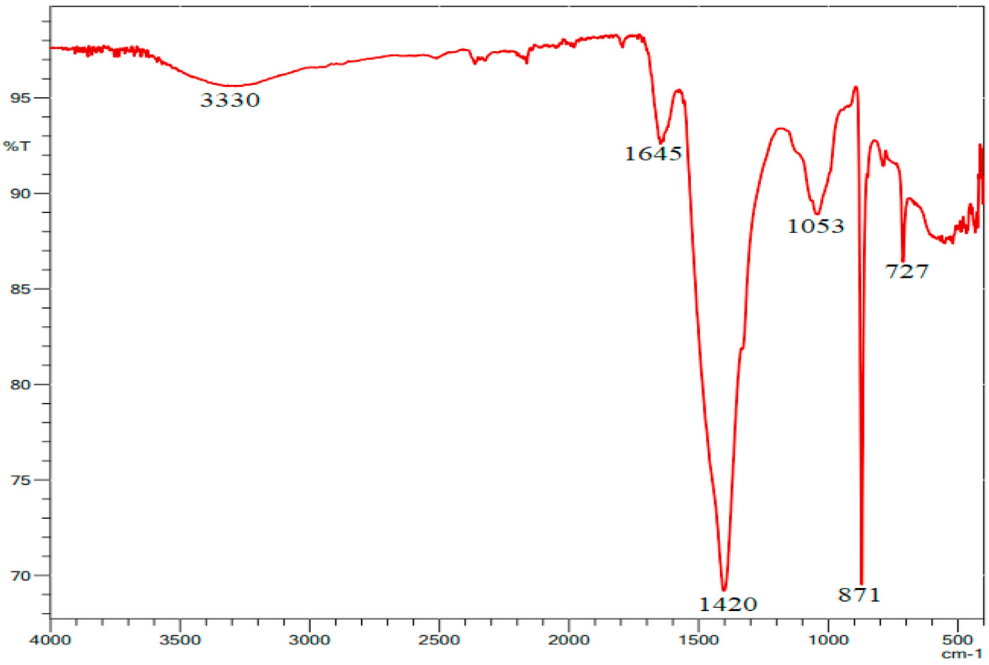

Fig. 3 – IR spectra of carbonatisation cake.

phosphorus removal tests were carried out. The results of the chemical oxygen demand tests performed in the filtrate solutions are given in Table 3. When the carbonatisation cake was in contact with water at a dose of 1 g L^{-1}, the COD of water was about 85.6 mg-O_2 L^{-1}.

These results indicate that some organic substances in the carbonatisation cake are released into the water environment. However, calcining the carbonatisation cake yielded a COD value of 0.09 mg-O_2 L^{-1} at 600 °C. The COD value decreased about 950 times as the calcination temperature increased. This shows that the organics released from the carbonatisation cake to the water were degraded during the heating of the cake.

The XRD and FTIR spectra of the carbonatisation cake and its calcines are given in Figs. 1 and 2. The peaks in the X-ray diffractogram were compared with the characteristic peaks in

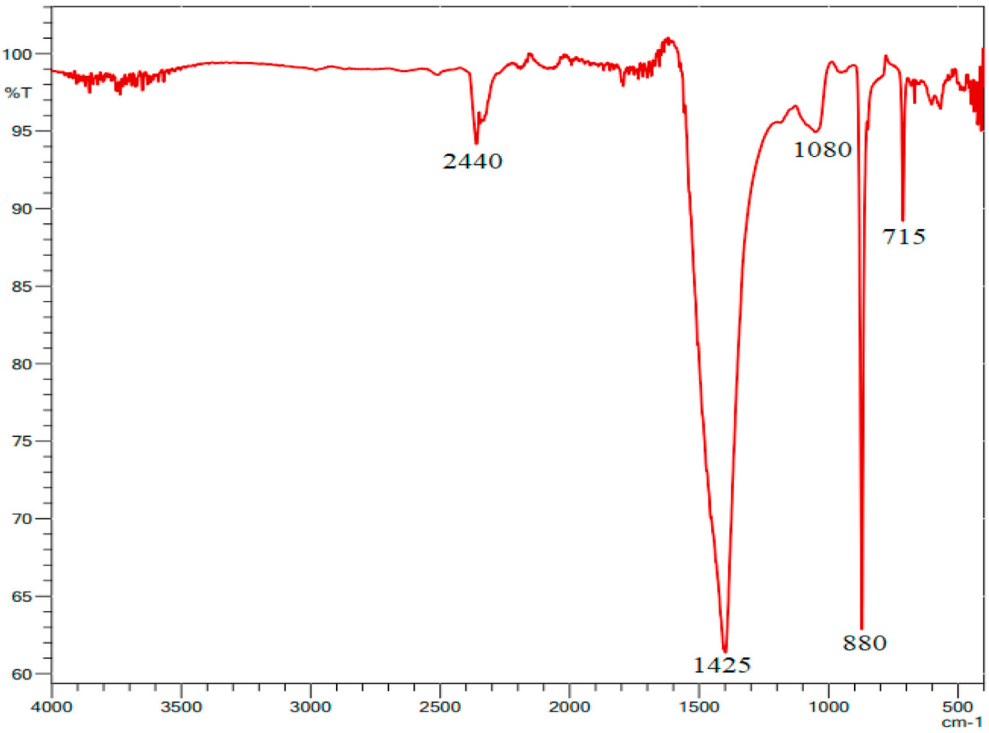

Fig. 4 – IR spectra of the product obtained by calcining the carbonatisation cake.

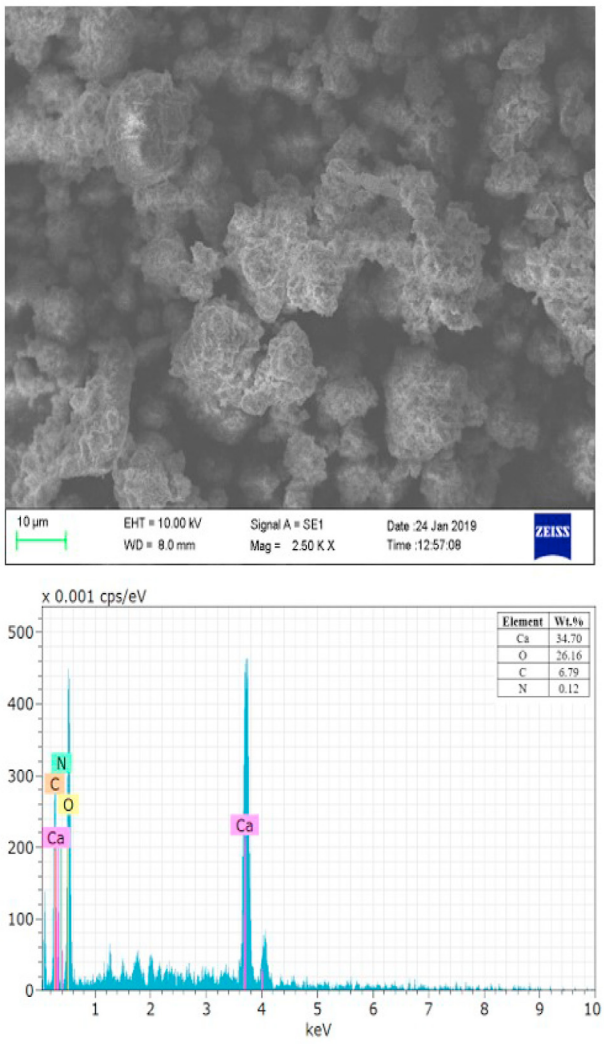

Fig. 5 – SEM image and EDX evaluation of carbonatisation cake.

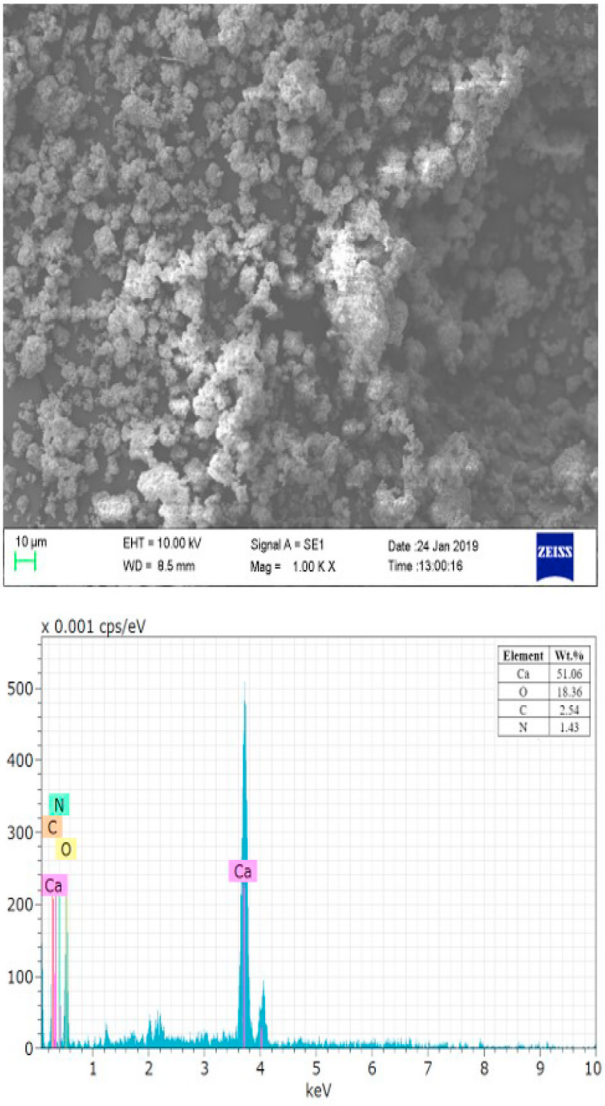

Fig. 6 – SEM image and EDX evaluation of calcined product.

Table 4 of the calcium carbonate compound in the literature. The peaks of the carbonatisation cake and calcined product coincided with all the peaks of calcium carbonate. It was also confirmed that the calcined product did not contain a crystalline component other than calcium carbonate. Moreover, the increase in the XRD peaks of the calcined product carbonized at elevated temperatures of organic substances was present in the environment. As a result, the XRD graph of the calcined product shows the formation of calcium carbonate almost pure [25,26].

In the IR spectrum of the carbonate cake and calcined carbonatisation cake, 717; 871; 1427; The observation of peaks observed in the 1789 and 2522 cm^{-1} wave numbers in the literature with calcium carbonate indicates that the carbonate cake and calcined product are composed of calcium carbonate. There are significant structural changes after 600 °C. This supports the results of thermal analysis and shows that calcium oxide is formed above 600 °C. The peak (Fig. 3) around 3448 cm^{-1} waveform in the carbonatisation cake does not appear calcined in Fig. 4. Since peaks obtained between 3300 and 3600 cm^{-1} generally belong to the hydroxyl group, the result can be attributed to the removal of the crystal water, especially in the carbonatisation cake. It may also be possible to decompose organic substances with functional hydroxyl groups in the carbonatisation cake. 1643 cm^{-1} wave count of the carbonatisation cake observed in the number of peaks was not observed in the calcined product, suggesting that this peak belongs to organic groups [27,28]. This indicates that the organics burn off completely. COD analysis also shows that calcine does not release organic matter to the aqueous medium (Table 3).

Figs 5 and 6 show the carbonatisation cake and calcined product in small particles from. The EDX analysis shows that the structure contained calcium compounds and that the calcined product increased by weight. The combustion of organics in the carbonatisation cake can be interpreted as the enrichment of inorganic compounds. The carbonate cake had a particle size <30 µm. The fact that the carbonatisation cake formed as a very small particle in a relatively basic environment suggests that it can be an effective adsorbent [29] (Fig. 7).

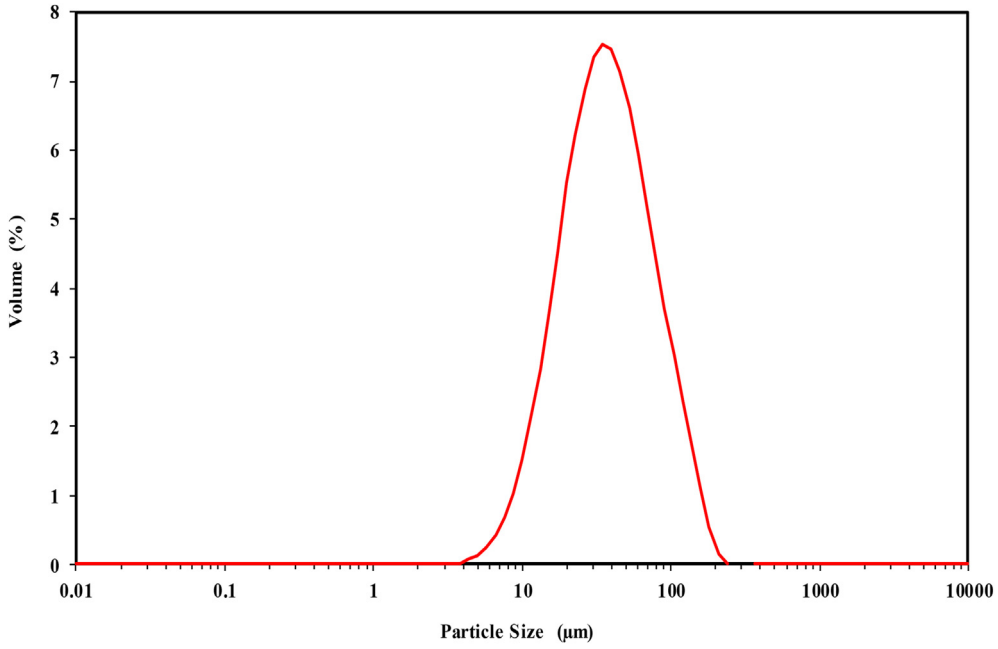

Fig. 7 – Particle size distribution of carbonatisation cake.

The TGA-DTA analyses of both substances are given in Figs. 8 and 9 to compare the structure of the carbonatisation cake with that of the calcined product. The calcination of the calcined product markedly increased at 690 °C. Fig. 9 shows that the pure calcium carbonate in the literature was identical with TGA-DTA. This result suggests that the calcined carbonatisation cake is pure calcium carbonate. The weight reduction of the carbonating cake occurs at a certain speed up to about 380 °C. About 12.5% weight reduction in this region is due to the removal of bound water and volatile organics. The weight reduction between 380 and 690 °C is very low. It can, therefore, be stated that the remainder of the organics was condensed and carbonated at the limit and that calcium carbonate calcination started. The weight loss in this region was about 5%. A rapid weight reduction of about 30% between 700 and 900 °C is related to the calcination of calcium carbonate. Therefore, the total weight reduction of 45.2% in the sample determined using thermal gravimetry is in harmony with the 43.8% reduction in the calcined product weights at 800 °C determined using chemical analysis (Tables 1 and 3) [30–32].

The results of the differential thermal analysis of the carbonatisation cake show that crystalline or capillary water is removed between 140 and 200 °C. Since the nitrogen gas in the

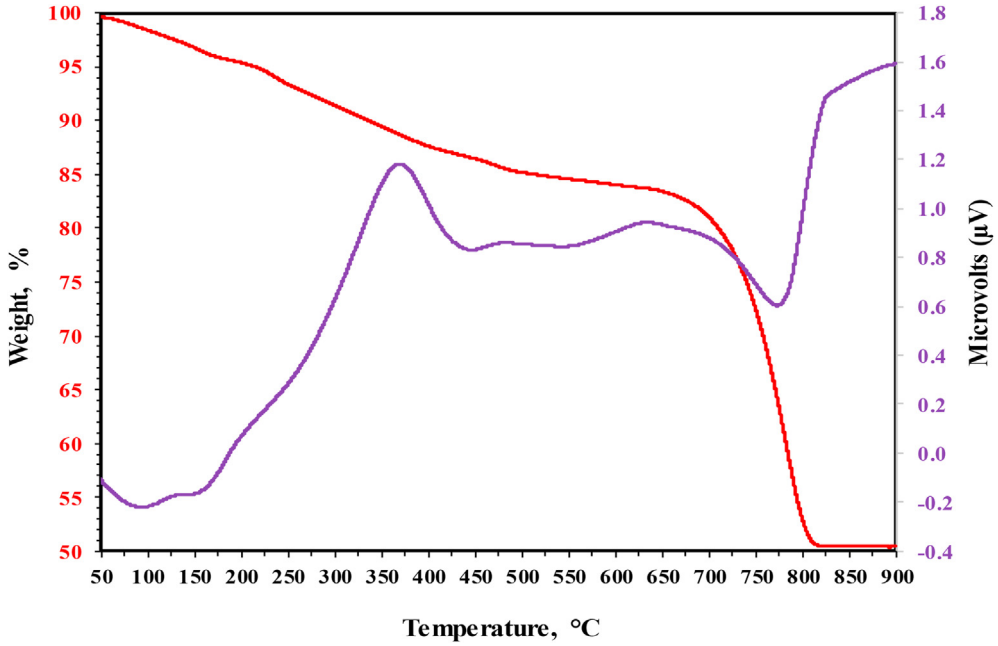

Fig. 8 – TGA-DTA diagram of carbonatisation cake.

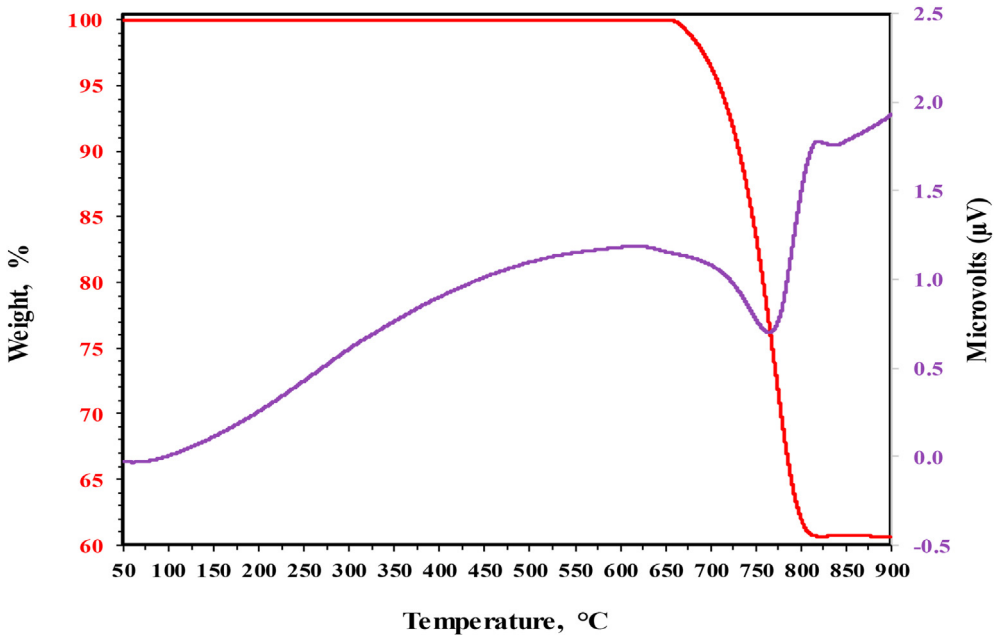

Fig. 9 – TGA-DTA diagram of calcined product.

device contains a little oxygen, the organic combustion is predominant in the region until about 400 °C and the decarboxylation, decarbonylation and dehydrogenation events occur at the same time. The expected calcination is observed at higher temperatures. The IR, TGA and DTA findings support the weight loss and changes in color in the calcination of the carbonatisation cake and comments of the calcines for the COD values given to the water.

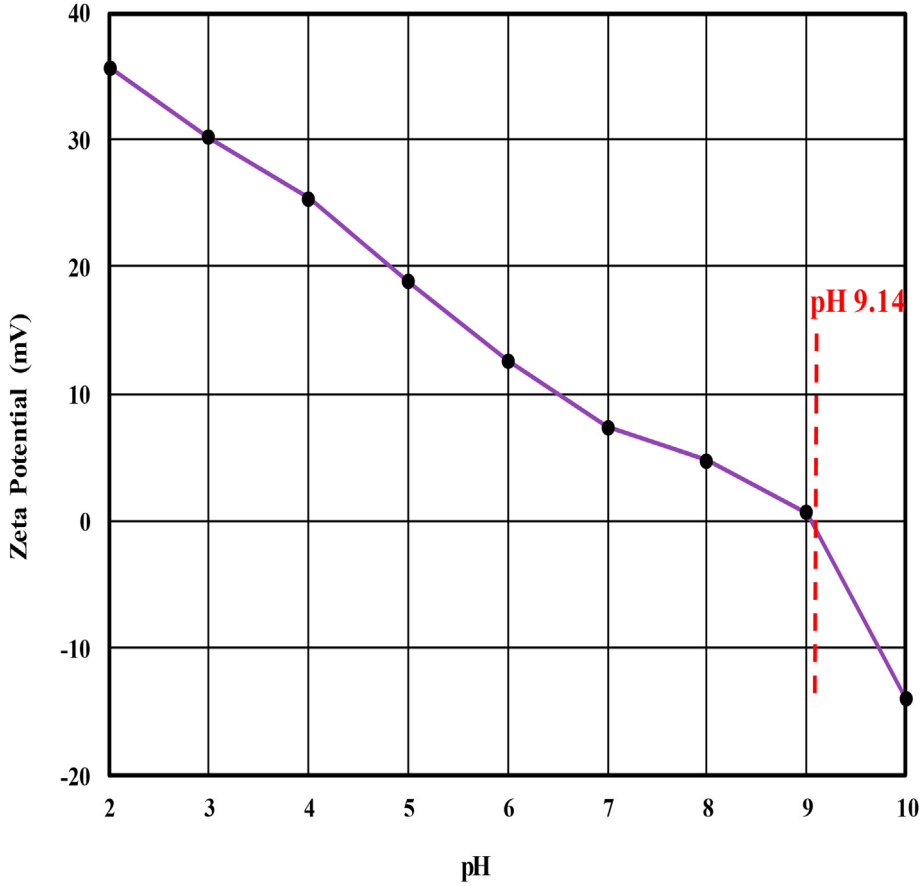

Fig. 10 – PH_{zpc} diagram of calcined product.

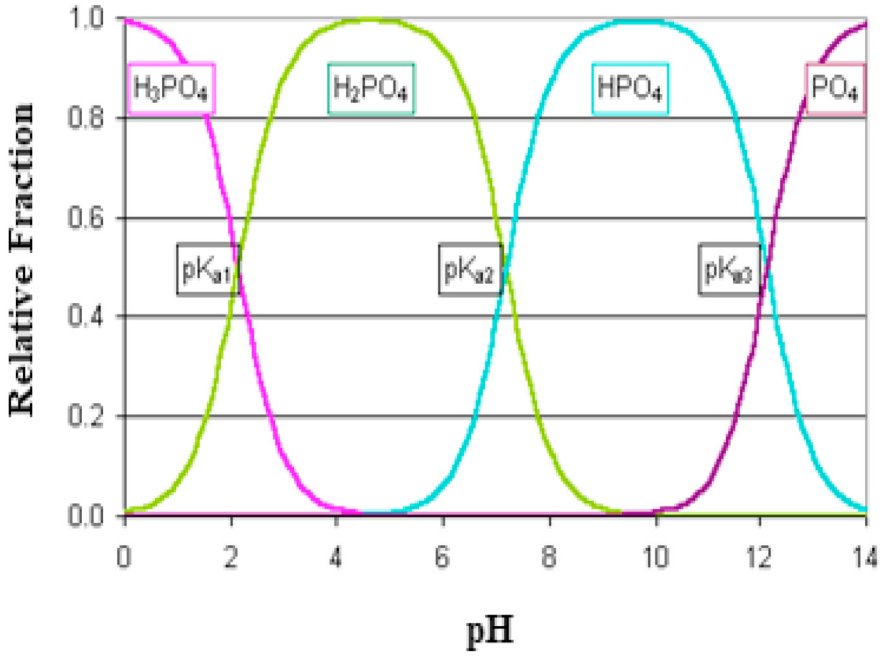

Fig. 11 – Distribution diagram for phosphate present as different protonated species as a function of pH.

3.2. *Adsorption mechanism*

Oxides and silicates are generally utilized as adsorbents due to low solubility and simplicity in adsorption. pH plays a critical role in adsorption (Fig. 16) because it determines the nature and content of orthophosphate and hydrolysis products on calcined carbonatisation cake surface. In this case, the solution consists of calcined carbonatisation cake hydrolysis reactions, orthophosphate species and ionic species. These reactions determine their electrokinetic and physicochemical properties and behavior in solution [33].

Zeta-calcined carbonatisation cake measurements in water indicate that the zero charge point of the mineral is realized at pH 9.14 (Fig. 10). With the addition of 50 mg L^{-1} PO_4^{3-}, the pH of the solution was 7.65. Species with orthophosphate are chemically adsorbed to the calcined carbonatisation cake for pH values greater than 7.65. Electrostatic and chemical interactions causes adsorption above pH 7.65. As a result, the identification of orthophosphate species of the solution and hydrolysis reactions at the surface of the calcined carbonatisation cake should be considered to elucidate the adsorption mechanism [12,34–36].

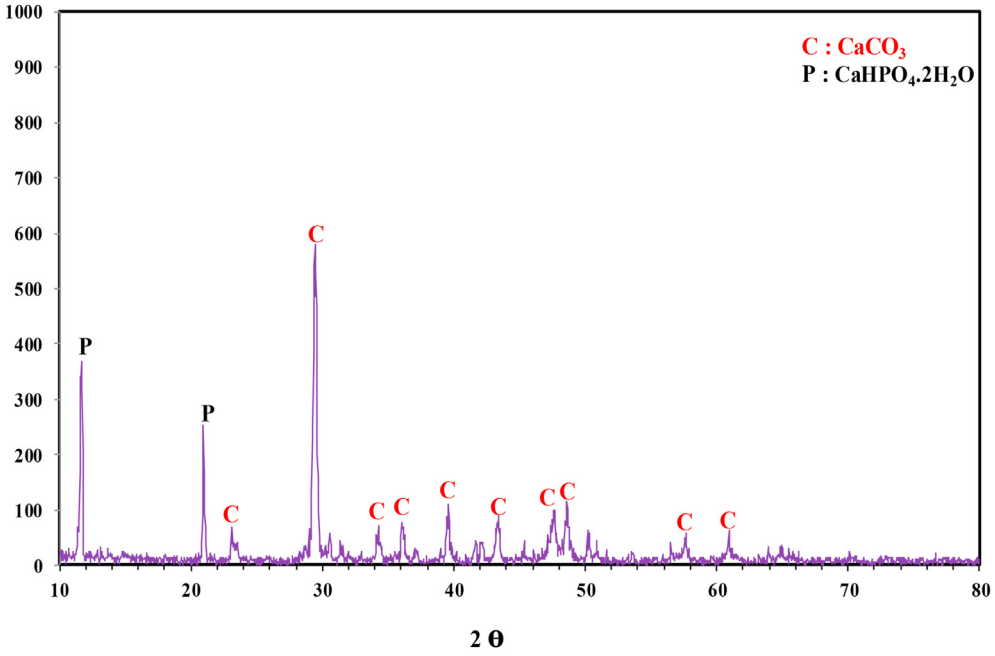

Fig. 12 – XRD graph after phosphate adsorption of calcined carbonatisation cake.

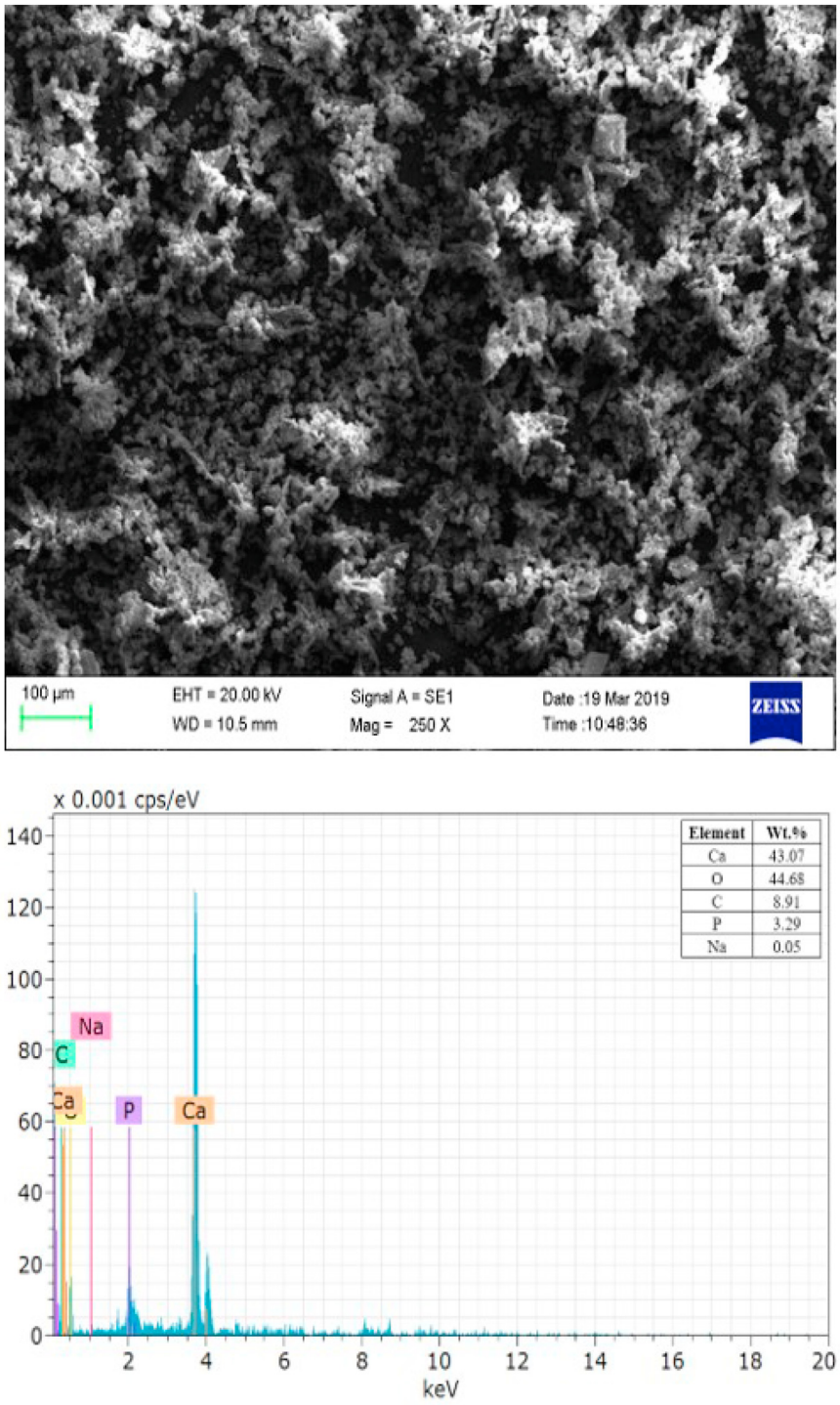

Fig. 13 – SEM image and EDX evaluation of the calcined carbonatisation cake after phosphate adsorption.

The properties of orthophosphates are explained using the following reactions with the pK perspectives at 25 °C [37,38],

$$PO_4^{3-} + H_2O \rightarrow HPO_4^{2-} + OH^- \ , pK = 1.68 \quad (3)$$

$$HPO_4^{2-} + H_2O \rightarrow H_2PO_4^- + OH^- \ , pK = 6.79 \quad (4)$$

$$H_2PO_4^- + H_2O \rightarrow H_3PO_4 + OH^- \ , pK = 11.67 \quad (5)$$

$$H_2O \rightarrow H^+ + OH^- \ , pK = 14.00 \quad (6)$$

Fig. 11 shows the protonation reactions (3)–(6), suggesting that the pH of $H_2PO_4^-$ and HPO_4^{2-} species ranges from 5 to 10. The content of $H_2PO_4^-$ is higher at pH < 7 whereas HPO_4^{2-} are valid at 7 < pH < 10. In Fig. 11, HPO_4^{2-} is superior to PO_4^{3-} species. The content of PO_4^{3-} is apparent and higher than that of HPO_4^{2-} at pH > 12.5 [39,40].

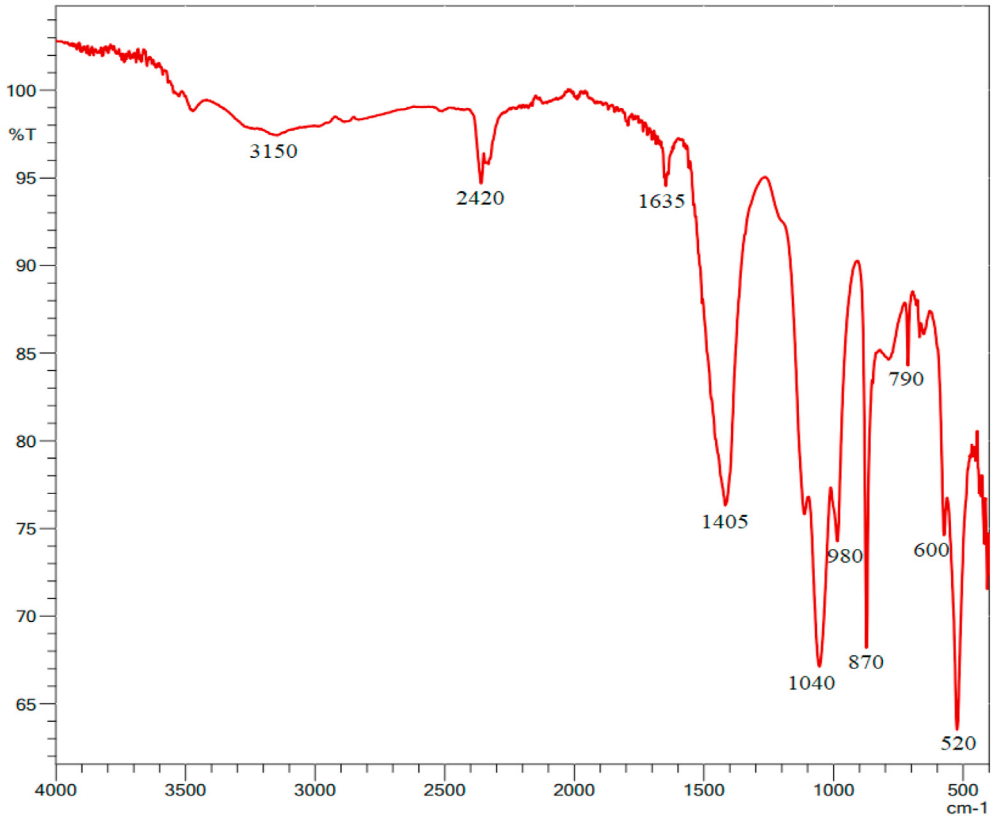

Fig. 14 – FTIR graph after phosphate adsorption of calcined carbonatisation cake.

pH is positively charged to the mineral surface at pH < 9. The negative species dominate at pH > 9, however, the content of positive species is still noteworthy. Some hydrolysis reactions for cationic and anionic species are given below:

$$CaCO_3 \rightarrow Ca^{2+} + CO_3^{2-}\ ,\ pK = 3.25 \quad (7)$$

$$CO_3^{2-} + H_2O \rightarrow HCO_3^{-} + OH^{-}\ ,\ pK = 3.67 \quad (8)$$

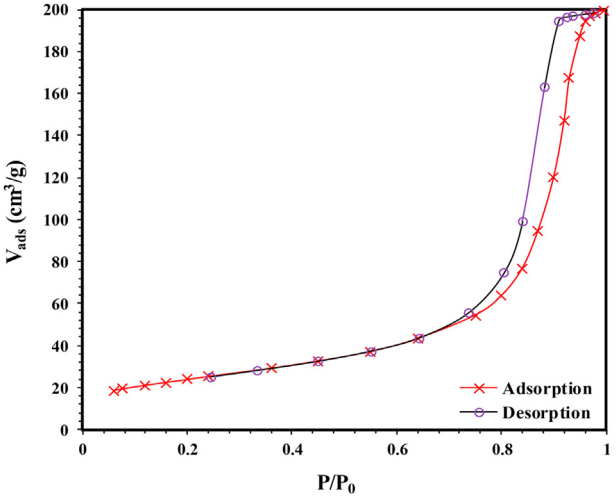

Fig. 15 – Nitrogen adsorption isotherm of the calcined carbonatisation cake.

$$Ca^{2+} + HCO_3^{-} \rightarrow CaHCO_3^{+}\ ,\ pK = -0.82 \quad (9)$$

$$Ca^{2+} + OH^{-} \rightarrow CaOH^{+}\ ,\ pK = -1.40 \quad (10)$$

Therefore, adsorption can possibly be explained using reactions (11) (12) and (13) on the surface of the calcined carbonatisation cake.

$$Ca^{2+} + H_2PO_4^{-} \rightarrow CaH_2PO_4^{+}\ ,pK = -1.08 \quad (11)$$

$$Ca^{2+} + HPO_4^{2-} \rightarrow CaHPO_4\ ,\ pK = -7.0 \quad (12)$$

$$Ca^{2+} + PO_4^{3-} \rightarrow CaPO_4^{-}\ ,\ pK = -6.5 \quad (13)$$

These results show that the specific adsorption of orthophosphate species on the surface of the calcined carbonatisation cake is the driving mechanism of orthophosphate intake from solution using calcium carbonate as the adsorbent, which corresponds to the findings of zeta-potential measurements (Fig. 10). It is also confirmed by the results of XRD and SEM-EDX analysis of the calcined carbonatisation cake (Figs. 12 and 13), which clearly shows that phosphate species are adsorbed on the surface of the calcined carbonatisation cake. The two major peaks of the calcined carbonatisation cake from the XRD graph are approximately 10 and 20, 2 theta angles of calcium hydrogen phosphate relative to the pre-adsorption XRD graph (Fig. 12). In addition, EDX findings clearly showed the presence of phosphorus. This mechanism

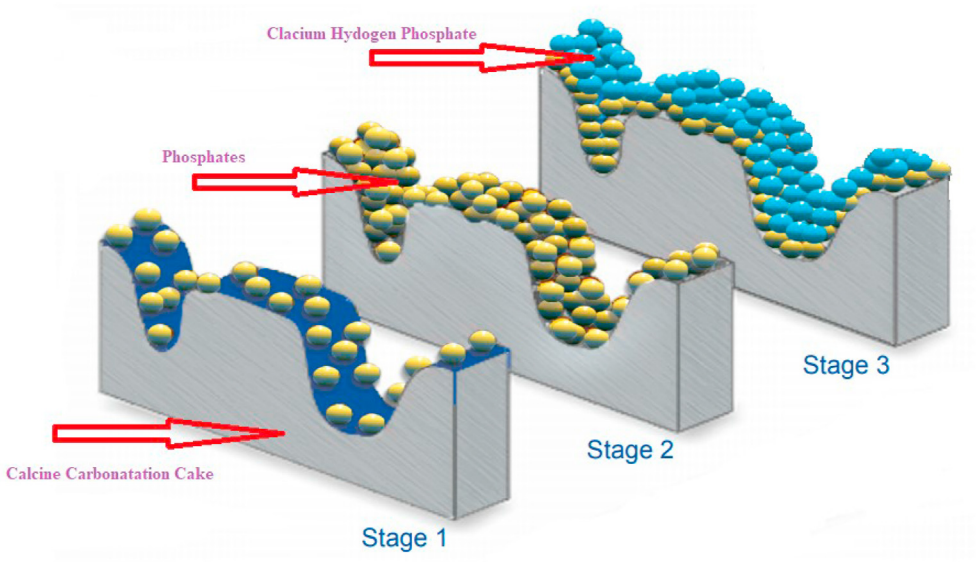

Fig. 16 – Phosphate adsorption mechanism.

tends to, to some extent, make the surface of the calcined carbonatisation cake similar to that of apatite [39–41].

The post-adsorption composition is also confirmed by the obtained IR spectra. Fig. 14 presents the typical IR-spectrum of calcium carbonate-phosphate samples with the absorption bands of the valence vibration of the absorption bands of the 525, 560, 600 cm^{-1} of PO_4^{3-} group. The symmetrical vibrations are the absorption bands of the deformation vibration of the 1400 cm^{-1} group of 865–870 and 960-980 cm^{-1} and the asymmetric vibrations 1040–1050 and 1100 - 1130 cm^{-1}. The absorption band 1630 - 1650 cm^{-1} refers to the deformation vibrations of the water groups. The suction band 3150, 3480 cm^{-1}, refers to the valence vibration of water and characterizes the presence of crystallization water. There was no difference between the IR-spectra of calcium carbonate-phosphate specimens and $CaHPO_4.2H_2O$. It was found that the suction bands of the brushite, PO_4^{3-} 530, 575, 600 cm^{-1} group, the absorption bands of the symmetrical vibrations 790, 870 and 985 cm^{-1} and the asymmetric vibrations 1060 to 1135 and 1210 cm^{-1}, as well as the 1645 cm^{-1} deformation vibration in the OH^- group characterize the absorption bands [25].

The BET surface area of the calcined carbonatisation cake was 83.75 $m^2\ g^{-1}$. Reversible Type II isotherm is the normal isotherm form obtained with a low or macroporous adsorbent surface area (Fig. 15) [42]. It is obvious that phosphate ions are adsorbed to the pores as well as calcium hydrogen phosphate is adsorbed on the surface. Phosphate removal mechanism is given in Fig. 16 (Schematic representation of different stages of phosphate mineralization directed to the surface. In step 1, the phosphates before the adsorption are in equilibrium with the ions in the solution. Phosphates approach a surface with chemical functionality. In step 2, phosphate before adsorption is collected near the surface of the calcined product in solution. In step 3, it causes more aggregation to the surface and adsorption/precipitation).

Consequently, the removal of orthophosphates from aqueous solution appears to be effective by adsorption of the calcined carbonatisation cake, leading to a decrease and/or eradication of environmental damage. No additional treatment of the adsorbed phosphate product of the calcined carbonatisation cake is required, therefore, it can be utilized as fertilizer for acidic soils as well.

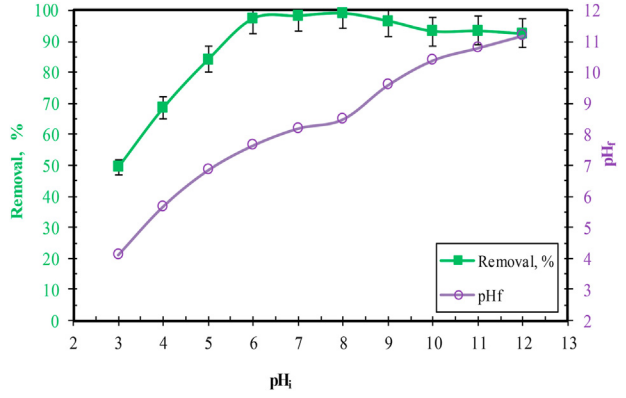

Fig. 17 – Effect of initial pH on phosphate removal.

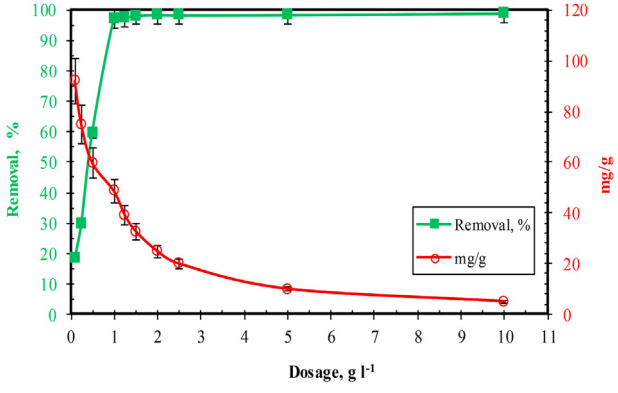

Fig. 18 – The effect of calcined carbonatisation cake dose on phosphate removal.

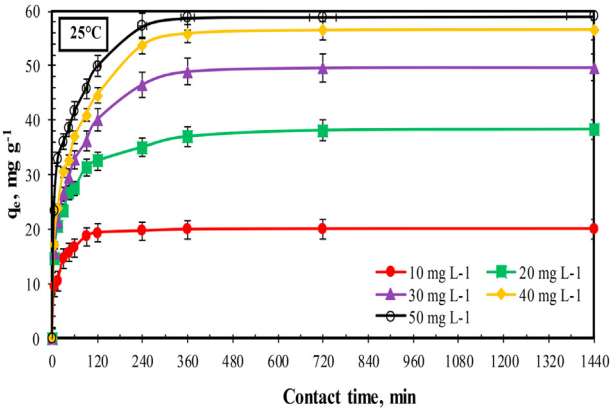

Fig. 19 – Effect of contact time on the removal of phosphate.

3.3. *Phosphate adsorption studies with calcined carbonatation cake*

The effects of pH, contact time, initial concentration, temperature and calcined carbonatisation cake dose on the removal of phosphates by the calcined carbonatisation cake were investigated.

3.3.1. *Initial pH*

Fig. 17 shows the final pH values from the experiments performed at different initial pHs. The final pH values range from 3 to 6 when the initial pH of the solutions is increased. Some pH values decrease at basic pH. The final pH values are higher than the initial ones. Table 1 shows that the calcined carbonatisation cake used is basic [12].

Therefore, the calcined carbonatisation cake removes the acidity of the solution and brings it to the basic area. The final pH of the 50 mg L^{-1} phosphate-containing solution prepared without any acid is about 7.65. No acid-base addition was, therefore, made in the next part of the study.

3.3.2. *Calcined carbonatisation cake dosage*

The effect of the calcined carbonatisation cake dose on the removal of phosphate from the solution at 50 mg L^{-1} is given in Fig. 18, showing that the higher the calcined carbonatisation cake dose, the higher the phosphate removal rate. For example, when the calcined carbonatisation cake was 0.1 g L^{-1}, 1 g L^{-1} and 10 g L^{-1}, the percentage of phosphate removed was 18%, 97% and 99%, respectively. Therefore, 0.5 g L^{-1} calcined carbonatisation cake dose was used in the following experiments [12,43].

3.3.3. *Contact time and initial phosphate concentration (IPC)*

Equilibrium time is an important factor in adsorption. Adsorption slows down when contact time goes up because there are fewer vacant active sites. This is associated with the chemical features of the surface as well [44–46]. Fig. 19 presents the contact time-dependent changes in the adsorption capacity (AC) (q) at 10 < initial concentrations < 50 mg L^{-1}. The IPC, content of calcined carbonatisation cake and temperature were, 0.5 g L^{-1} and 25 °C, respectively. Fig. 18 suggests that more phosphate was adsorbed on the calcined carbonatisation cake when contact time was longer, achieving an equilibrium faster at lower IPCs. Phosphates uptake was fast in the first hour. Afterwards, it continued slowly till an equilibrium in 180 min, and then, was almost steady. When the IPC was raised from 10 to 50 mg L^{-1}, the equilibrium adsorption capacity went up from 19.96 to 59.08 mg g^{-1}, suggesting that initial concentration has a great effect on AC. On the other hand, there was no increase in the AC with a further increase in the IPC because of the active sites on the calcined carbonatisation cake.

3.3.4. *Temperature*

Experiments were performed at 25, 45 and 55 °C. The IPC, calcined carbonatisation cake dosage and time were 50 mg L^{-1}, 0.5 g L^{-1} and 1440 min, respectively. According to the findings, the phosphate AC of the calcined carbonatisation cake went up from 59.08 to 91.57 mg g^{-1} with an increase

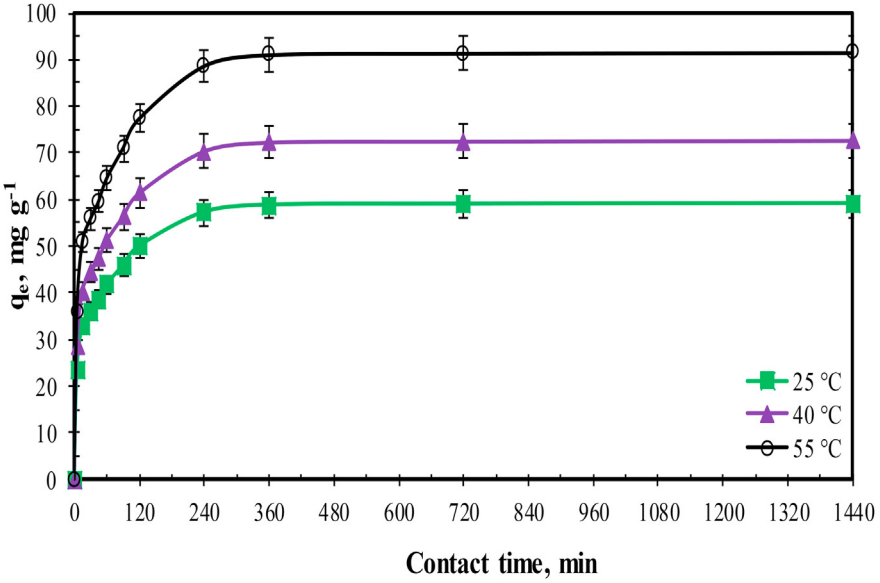

Fig. 20 – Effect of temperature on the removal of phosphate.

Table 5 – Calculated model parameters and regression coefficients for pseudo-first-order, pseudo-second-order and intraparticle diffusion models for various temperatures.

Kinetic models	Parameters	Temperature		
		25 °C	40 °C	55 °C
Pseudo First Order	Equation	y = −0.0228x+4.042	y = −0.0191x+3.205	y = −0.0254x+3.7038
	k_1 (l min^{-1})	0.028	0.0191	0.0254
	q_{cal} (mg g^{-1})	36.81	54.61	70.51
	R^2	0.9443	0.9698	0.9795
	X^2	8.40	4.49	4.84
Pseudo Second Order	Equation	y = 0.0015x+0.2297	y = 0.0018x+0.1905	y = 0.0023x+0.1171
	k_2 (g (mg.min)$^{-1}$)	0.0015	0.0018	0.0023
	q_{cal} (mg/g)	60.04	73.19	91.92
	R^2	0.9915	0.9969	0.9956
	X^2	0.016	0.0037	0.0014
Intra Particle Diffusion	First Equation	y = 0.2219x+20.55	y = 0.2514x+30.78	y = 0.4757x+45.72
	k_{dif} (mg (g.$min^{0.5}$)$^{-1}$)	0.2219	0.2514	0.4757
	q_{cal} (mg/g)	49.55	65.78	86.72
	R^2	0.9814s	0.9859	0.9865
	X^2	1.54	0.65	0.26
q_{exp} (mg g^{-1})		59.08	72.67	91.56

in temperature from 298 to 328 K for a contact time of 240 min (Fig. 20). The increase in adsorption efficiency with temperature indicated that adsorption was endothermic [47].

3.3.5. *Adsorption kinetics*

The kinetic behavior of the phosphate solution-calcined carbonatisation cake was identified using pseudo-first-order (PFO), pseudo-second-order (PSO) and intraparticle diffusion (ID) equations.

The first order adsorption rate expression based on the solid phase concentration in the adsorption processes in solid–liquid phase systems was first demonstrated by Lagergren. It is therefore also referred to as the Lagergren equation [48]. Accordingly, for an adsorption process in solution, the equation is as follows:

$$\ln(q_e - q) = \ln q_e - k_1 t \quad (14)$$

where qe (mg/g) shows the amount of the adsorbed substance in equilibrium and q (mg g^{-1}) shows the amount of adsorbed substance at any t moment. k_1 (l/min) is the first order adsorption rate constant. Using the data obtained from experimental data, the correlation coefficient of the linear graph drawn between log (q_e-q) values and t is close to 1, and the conformity of the process to the first order speed expression is determined. The speed constant k1 is calculated from the slope of the line.

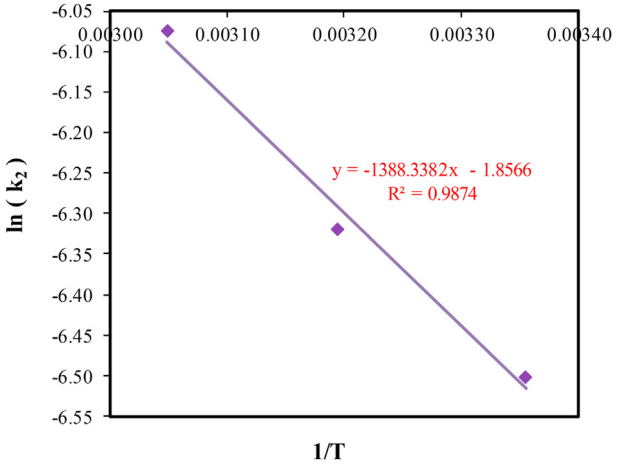

Fig. 21 – ln k vs. 1/T plot for phosphate adsorption on calcine carbonatisation cake.

$$\frac{t}{q} = \frac{1}{k_2 q_e^2} + \frac{t}{q_e} \quad (15)$$

The second order speed expression can be written as [49]. In this equation k_2 (g/mg. Min) is the second order adsorption rate constant. According to the data obtained from an adsorption process, the correlation coefficient of the linear graph drawn between 1/(q_e-q_t) and t is close to 1. The k_2 value can be found from the slope of the graph.

One of the mechanisms of adsorption is the diffusion model [50].

$$q = k_i t^{1/2} + I \quad (16)$$

q: the concentration of adsorbed substance at time t (mg g^{-1}); k: diffusion rate constant [mg/(g $dk^{1/2}$)]. By this equation, the slope of the linear graph drawn between q and $t^{1/2}$ gives k_i, and the slipping gives I.

Time data were used in the PFO, PSO and ID. Regression analysis was performed to choose the most suitable one [51]. Table 5 shows the kinetic parameters, equations and regression coefficients for the PFO, PSO and ID. Experimental q_e in Table 5 are the values at the second point of the flat plateau region in the evaluation graphs not given here. According to Table 5, the PSO was the most suitable equation for the experimental data.

After the experimental data are applied to the kinetic models, the speed constant of the most suitable model is considered to be the adsorption rate constant (k_{ad}). There are activation energies for the respective model that establishes a link between k_{ad} values and temperature for different

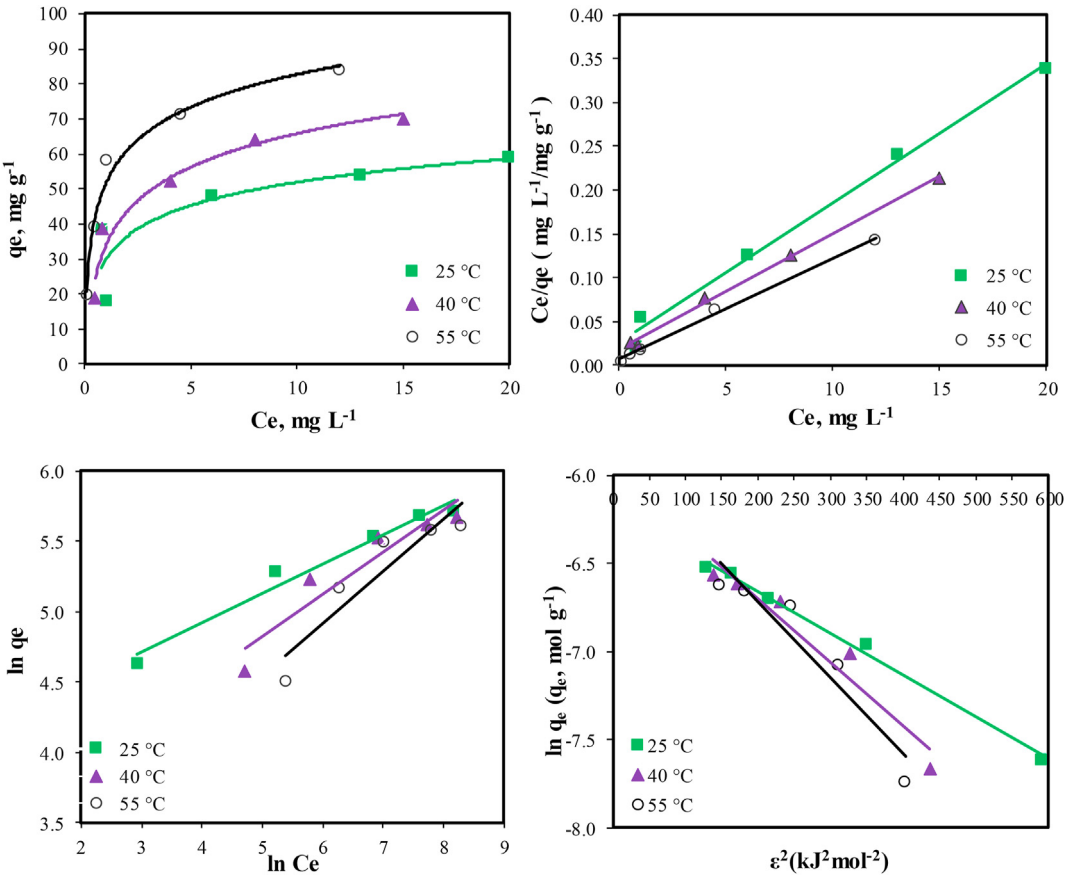

Fig. 22 – Isotherm Plot for phosphate sorption by calcine carbonatisation cake (a, Non-linear; b, Langmuir; c, Freundlich; d, Dubinin-Radushkevich (DR) isotherms).

concentrations at various temperatures. For this purpose, the equilibrium of 17 is obtained by taking the logarithm of the two lines, and the activation energy is obtained from the slope of the line drawn between lnk and 1/T (Fig. 21).

$$k_{ad} = A\left(e^{-E_A/RT}\right) \quad (17)$$

where k_{ad} is the adsorption rate constant, A is the frequency factor and Ea is the activation energy. For these parameters, units may vary depending on the unit of the rate constant. Activation energy can be calculated, for example kJ mol^{-1}.

AE magnitude might give some idea about the physical or chemical characteristics of adsorption. Physical adsorption needs no great volume of AE for Van Der Waals forces, which are not higher than 1 kcal mol^{-1} (4.18 kJ mol^{-1}), are clear from adsorption. On the other hand, chemical adsorption needs stronger forces. It is chemical at $2<E_a<20$ kcal mol^{-1} (8.4 and 83.7 kJ mol^{-1}) [52,53].

The data were in conformity with the simple II order kinetic model. The temperature data for 10–50 mg L^{-1} phosphate initial concentrations were applied to this model. The activation energy from the Arrhenius equation for 10–50 mg L^{-1} phosphate solutions was 11.54 kj mol^{-1}.

3.3.6. *Adsorption isotherms*

The equilibrium data are applied to different types of isotherm which can be converted into linear form to elicit useful information. Adsorption data are often assessed based on the Freundlich, Langmuir and D-R adsorption isotherms.

In a nonlinear adsorption graph of L-type isotherm, saturation is attained at high adsorbate concentrations, that is, q_e attains monolayer saturation [50] suggesting that Langmuir equation is suitable for measuring parameters [54].

Langmuir isotherm is better than the other isotherms at determining whether the retention in active adsorption areas on solid surfaces is physical or chemical. In Langmuir

Table 6 – Calculated isotherm parameters for phosphate sorption by calcine carbonatisation cake.

Temperature °C	Langmuir			Freundlich			D-R		
	b (l mg^{-1})	q_{max} (mg g^{-1})	R^2	1/n	K_f ((mg g^{-1}) (l mg)$^{-1/n}$)	R^2	q_{max} (mg g^{-1})	E (kJ mol^{-1})	R^2
25	0.0323	65.16	0.9917	0.4715	15.261	0.9613	80.74	6.79	0.9799
40	0.0417	79.75	0.9952	0.4369	19.961	0.9449	99.42	7.25	0.9665
55	0.0506	96.14	0.9904	0.4148	24.939	0.9529	125.14	7.87	0.9789

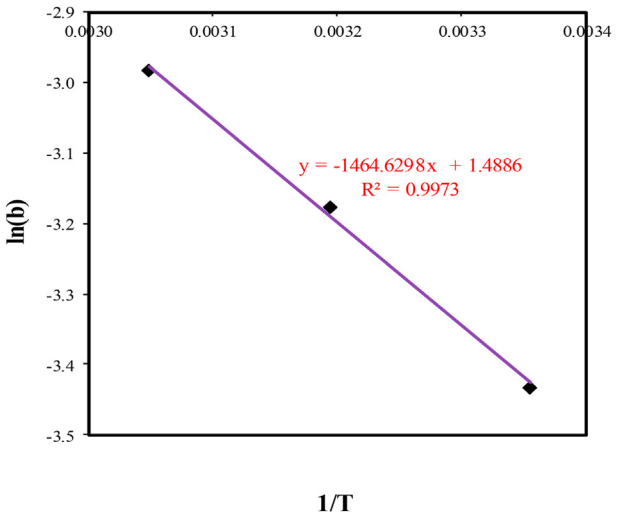

Fig. 23 – ln b vs. 1/T plot for phosphate adsorption on calcine carbonatisation cake.

isotherm, adsorption increases linearly with the initial concentration of the adsorbate. At highest saturation, the surface is covered with one layer and the content of the adsorbate adsorbed to the surface remains constant [55].

$$\frac{C_e}{q_e} = \frac{1}{b.q_m} + \frac{C_e}{q_m} \tag{18}$$

where qmax is the maximum AC (mg g^{-1}); b is a constant associated with the adsorption energy, (L mg^{-1}). When q/qe versus Ce is plotted, qmax and b values can be calculated from the slope and offset of the line obtained.

According to Freundlich, suitable sites for adsorption on an adsorbent surface are heterogeneous containing adsorption sites of different types. The Freundlich isotherm indicates that the amount of adsorbent adsorbed in a given amount rapidly increases with increasing concentration initially but increases slowly when the solid surface is saturated. Freundlich isotherm [56];

$$lnq_e = \frac{1}{m} lnC_e + lnK_f \tag{19}$$

q_e is the adsorbed substance amount (mg); m is the amount of adsorbent (g) and C_e is the equilibrium concentration (mg L^{-1}) of the adsorbent in solution. K_f (mg g^{-1}) is the Freundlich constant, which is a measure of AC. The other Freundlich constant n is dimensionless.

The equilibrium data used in the DR equation [57],

$$lnq_e = lnq_m - \beta\varepsilon^2 \tag{20}$$

where q_m is the highest adsorbate concentration adsorbed onto the unit weight of the adsorbent (mg g^{-1}), β is the constant associated with adsorption energy (mol^2 kJ^{-2}) and ε is the Polanyi potential, that is equal to $RT\ ln(1 + 1C_e^{-1})$. The plot of lnq vs. ε^2 points to a linear relation. The slopes of the DR plots give β constant, and q_m is calculated using the intercept of the plot [57].

A nonlinear isotherm graph was obtained using this data (Fig. 22), suggesting that the system reached saturation, indicating that the isotherm is an L type isotherm [51]. Accordingly, Freundlich, Langmuir and D-R isotherm applications of 10–50 mg L^{-1} phosphate starting concentrations and 1440 min of equilibration time are given in Fig. 22. In addition, some constants calculated using the isotherms are given in Table 6.

The results of the Freundlich, Langmuir and D-R isotherms indicate that the Langmuir isotherm is more suitable for this system. The calculations (Langmuir constant q_{max}) showed that the phosphate sorption capacity in the working conditions of calcined carbonatisation cake was 65.16–96.14 mg g^{-1}.

E (sorption energy) from the D-R isotherm is between 6.79 and 7.78 kJ mol^{-1} for 25, 40 and 55 °C. The sorption energy was between 0 and 8 kJ mol^{-1}, indicating that the process has adsorption characteristics. In this study, adsorption is dominant.

Thermodynamic parameters can also be calculated using the Langmuir constant. The thermodynamic parameters of adsorption such as free energy (ΔG°), enthalpy (ΔH°) and entropy (ΔS°) change can be calculated as described below and with the following equations. The energy parameter of adsorption, b, has the following relation with the adsorption enthalpy [51,58].

$$lnb = lnb_0 - \frac{\Delta H^\circ}{RT} \tag{21}$$

According to this equation, the lnb values are plotted according to the 1/T values, and the adsorption enthalpy change can be found from the slope of the line obtained.

$$ln\left(\frac{1}{b}\right) = \frac{\Delta G^\circ}{RT} \tag{22}$$

ΔG° is the free energy change (kJ mol^{-1}), T is the absolute temperature (K) and R is the universal gas constant (8.314 J $mol^{-1}K^{-1}$). b can also be expressed in the following equation, including the terms ΔH° (kJ mol^{-1}) and ΔS° (kJ $mol^{-1}K^{-1}$), as a function of T.

$$\Delta G^\circ = \Delta H^\circ - T\Delta S^\circ \tag{23}$$

ΔH° and ΔS° can be measured using the slope and offset of the straight line in the linear graph to be drawn between lnb and 1/T (Fig. 23).

The thermodynamic parameters calculated using Eqs (21)–(23) according to the b values calculated from Langmuir isotherm are shown in Table 7. According to these values, the enthalpy value is positive (ΔH = 12.18 kj mol^{-1}). The depletion of the calcined carbonatisation cake from aqueous solutions shows that it is endothermic. The negative change in free energy (ΔG = −8.505 kj mol^{-1}) indicates that sorption is spontaneous. Positive entropy change in small values

Table 7 – Thermodynamic parameters for phosphate sorption by calcine carbonatisation cake.

Temperature °C	ΔH (kj mol^{-1})	ΔG (kj mol^{-1})	ΔS (kj mol^{-1})
25	12.18	−8.505	0.0123
40		−8.268	
55		−8.137	

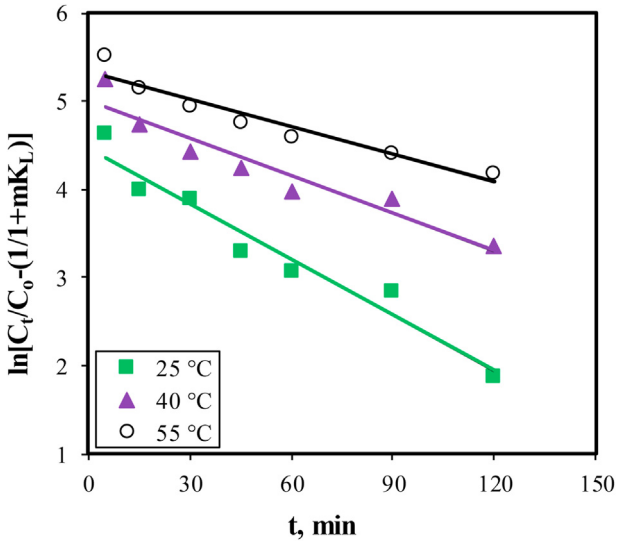

Fig. 24 – Graphs of t-ln [C/C$_0$- (1/1 + mK$_L$)] obtained at different temperatures for adsorption of the phosphate with calcined carbonatisation cake.

($\Delta S = 0.0123$ kj mol^{-1}) may be caused by an increase in irregularity in the sorbent interface and changes in the surface of the adsorbent during sorption.

3.3.7. *Mass transfer calculations for phosphate adsorption with calcined carbonatisation cake*

Gordon et al. [59] proposed that the general mass transfer obtained by some assumptions for adsorption is as in equality 24:

$$\ln\left(\frac{C}{C_0} - \frac{1}{1+m.K_L}\right) = \ln\left(\frac{m.K_L}{1+m.K_L}\right) - \left(\frac{1+m.K_L}{m.K_L}\beta_L s_s t\right) \quad (24)$$

where C_0 and C are the phosphate concentration (mg-P L^{-1}) at the beginning and end of contact at the solution, respectively, β_L is the surface transfer coefficient (cm min^{-1}), S_s is the volume based specific surface (cm^{-1}), K_L shows the Langmuir constant (cm^3 g^{-1}), and m shows the amount of adsorbent (g cm^{-3}) used per unit volume of solution. The ss and m values can be calculated using Eqs (11) and (12), respectively. Langmuir constant K_L is found by multiplying b and Q_o parameters.

$$m = W/V \quad (25)$$

$$s_s = \frac{6m}{d_p\rho(1-\varepsilon)} \quad (26)$$

where W is the amount of adsorbent (g), V is the solution volume (cm^3), d_p is the mean particle diameter (cm) and ε is the porosity of the adsorbent. ln [C/C$_0$- (1/1 + mK$_L$)] against the values of t is measured from the slope of the line obtained by plotting.

Table 8 – Calculated mass transfer and por diffusion coefficients for the adsorption of phosphate with calcined carbonatisation cake.

Temperature °C	$\beta_L \times 10^4$ (cm min^{-1})	D × 10^9 (cm min^{-1})
25	2.745	1.223
40	3.014	1.752
55	3.469	1.186

Table 9 – Adsorption capacities of some materials reported in literature.

Adsorbent	Adsorption capacity mg g^{-1}(q_m, mg/g)s	Reference
Fe–Mn–Zn Oxide nanocomposite	149.25	[4]
Nanostructured trimetal oxide	48.30	[62]
Bentonite	46.95	[63]
Mg/Al layered double hydroxide	81.83	[64]
Fe–Zr binary oxide	102.3	[65]
Alunite	118.0	[66]
Biochar/AlOOH	135.0	[67]
Fine dolomite	377.8	[68]
Calcine carbonatisation cake.	59.05	This study

The graph drawn to determine mass transfer coefficients at different temperatures for phosphate adsorption with calcined carbonatisation cake is shown in Fig. 24. It show that the initial distinct linearity is disrupted for a period of time. This is probably due to the fact that the mechanism of adsorption is initially differentiated, although the film diffusion is initially effective.

Boyd et al. [60] stated that diffusion coefficient can be calculated using the following equation:

$$t_{1/2} = 0.03\frac{r_0}{D} \quad (27)$$

where r_0 is the radius of the adsorbent particle (cm) and the D is the por diffusion coefficient (cm^2 min^{-1}). Equation $t_{1/2}$ is the half-life of the adsorption reaction. In this study, the diffusion coefficient was calculated using the following equation:

$$t_{1/2} = \frac{0.693}{k_a} \quad (28)$$

The mass transfer coefficients and por diffusion coefficients calculated for phosphate adsorption at different temperatures with calcined carbonatisation cake are given in Table 8.

The mass transfer coefficient increases with an increase in temperature. This is another indicator of phosphate adsorption with calcined carbonatisation cake. The por diffusion coefficient shows an irregular change in temperature. In this case, adsorption can be considered an indicator that diffusion control is not realized. Calculation of mass transfer and diffusion coefficients with the calcined carbonatisation cake for phosphate adsorption is supported by the change in temperature, kinetic and thermodynamic findings [61].

Numerous studies used adsorbents to remove phosphate and obtained operating parameters related to both kinetics and equilibrium. Table 9 (as Langmuir constant, q_m) shows that adsorption capacities in adsorption studies. The calcine carbonate cake used to remove phosphate had more AC than

most meaterials in Table 9. It shows that calcine carbonate cake can be used for phosphate removal from aqueous solutions.

4. Conclusion

A small granular cake was used to remove phosphate from aqueous solutions. The cake was the product of the filtration of carbonatisation sludge, which is a residue of the production of sugar from sugar beet. The cake contained 80–85% calcium carbonate on dry basis and the rest was organic material, which was degraded by burning at 600 °C in an oven. The COD analysis showed that the organic matter was completely removed by burning and that it caused no damage to the environment. The calcium carbonate content after calcination was 98.5%. According to the results of physicochemical tests, the specific surface area, porosity, mean particle size, pore diameter, apparent density, actual density and pHzpc were 83.75 $m^2\ g^{-1}$, 0.3074 cm^3, 15.33 μm and 142.38 Å, 1.058 and 1.984 g cm^{-3} and 9.14. The equilibrium data obtained at different temperatures were applied to different isotherms. The results showed that the data were compatible with the Langmuir isotherm. The positive value of the adsorption enthalpy showed that adsorption had a significant chemical character. The activation energy for the absorption of the phosphate with the calcined carbonatisation cake was 11.54 kj mol^{-1}. The mass transfer coefficient and por diffusion coefficient calculated for this process were $\beta_L = 2.745 \times 10^4$ and $D = 1.223 \times 10^9$ cm min^{-1}, respectively. It was determined that calcined carbonatisation cake is not only a phosphate treatment but a general treatment material. Since it is a reusable material and can substitute lime, it provides effective resource utilization. The phosphate adsorbed product of the calcined carbonatisation cake can also be used as fertilizer in the treatment of acidic soils.

Declaration of Competing interest

The author declare that there are no conflicts of interest regarding the publication of this paper.

REFERENCES

[1] Kuroki V, Bosco G, Fadini PS, Mozeto AA, Cestari AR, Carvalho WA. Use of a La (III)-modified bentonite for effective phosphate removal from aqueous media. J Hazard Mater 2014;274:124–31. https://doi.org/10.1016/j.jhazmat.2014.03.023.

[2] Diao J, Shao L, Liu D, Qiao Y, Tan W, Wu L, et al. Removal of phosphorus from leach liquor of steel slag: adsorption dephosphorization with activated alumina. J Min Met & Mater Soci. 2018;70(10):2027–32. https://doi.org/10.1007/s11837-018-3076-9.

[3] Xiong J, He Z, Mahmood Q, Liu D, Yang X, Islam E. Phosphate removal from solution using steel slag through magnetic separation. J Hazard Mater 2008;152(1):211–5. https://doi.org/10.1016/j.jhazmat.2007.06.103.

[4] Kondalkar M, Fegade U, Attarde S, Ingle S. Phosphate removal, mechanism, and adsorption properties of Fe-Mn-Zn oxide trimetal alloy nanocomposite fabricated via co-precipitation method. Sep Sci Technol 2019:1–13. https://doi.org/10.1080/01496395.2018.1550513.

[5] Fan R, Chen CL, Lin JY, Tzeng JH, Huang CP, Dong C, et al. Adsorption characteristics of ammonium ion onto hydrous biochars in dilute aqueous solutions. Bioresour Technol 2019;272:465–72. https://doi.org/10.1016/j.biortech.2018.10.064.

[6] Jang J, Lee DS. Effective phosphorus removal using chitosan/Ca-organically modified montmorillonite beads in batch and fixed-bed column studies. J Hazard Mater 2019;375:9–18. https://doi.org/10.1016/j.jhazmat.2019.04.070.

[7] Yoshida H, Galinada WA. Equilibria for adsorption of phosphates on OH-type strongly basic ion exchanger. AIChE J 2002;48(10):2193–202.

[8] Altundoğan HS, Tümen F. Removal of phosphates from aqueous solutions by using bauxite. I: effect of pH on the adsorption of various phosphates. J Chem Technol Biotechnol: Int Res Process Environ Clean Technol 2002;77:77–85.

[9] Altundoğan H, Tümen F. Removal of phosphates from aqueous solutions by using bauxite II: the activation study. J Chem Technol Biotechnol: Int Res Process Environ Clean Technol 2003;78:824–33.

[10] Li Y, Liu C, Luan Z, Peng X, Zhu C, Chen Z, et al. Phosphate removal from aqueous solutions using raw and activated red mud and fly ash. J Hazard Mater 2006;137:374–83. https://doi.org/10.1016/j.jhazmat.2006.02.011.

[11] Liu Y, Sheng X, Dong Y, Ma Y. Removal of high-concentration phosphate by calcite: effect of sulfate and pH. Desalin 2012;289:66–71. https://doi.org/10.1016/j.desal.2012.01.011.

[12] Karageorgiou K, Paschalis M, Anastassakis GN. Removal of phosphate species from solution by adsorption onto calcite used as natural adsorbent. J Hazard Mater 2007;139:447–52. https://doi.org/10.1016/j.jhazmat.2006.02.038.

[13] Li M, Liu J, Xu Y, Qian G. Phosphate adsorption on metal oxides and metal hydroxides: a comparative review. Environ Rev 2016;24(3):319–32. https://doi.org/10.1139/er-2015-0080.

[14] Liu H, Sun X, Yin C, Hu C. Removal of phosphate by mesoporous ZrO2. J Hazard Mater 2008;151(2–3):616–22. https://doi.org/10.1016/j.jhazmat.2007.06.033.

[15] Huang W, Wang S, Zhu Z, Li L, Yao X, Rudolph V, et al. Phosphate removal from wastewater using red mud. J Hazard Mater 2008;158(1):35–42. https://doi.org/10.1016/j.jhazmat.2008.01.061.

[16] Yin H, Yun Y, Zhang Y, Fan C. Phosphate removal from wastewaters by a naturally occurring, calcium-rich sepiolite. J Hazard Mater 2011;198:362–9. https://doi.org/10.1016/j.jhazmat.2011.10.072.

[17] Nguyen TAH, Ngo HH, Guo WS, Zhang J, Liang S, Lee DJ, et al. Modification of agricultural waste/by-products for enhanced phosphate removal and recovery: potential and obstacles. Bioresour Technol 2014;169:750–62. https://doi.org/10.1016/j.biortech.2014.07.047.

[18] Arslanoğlu H. Direct and facile synthesis of highly porous low cost carbon from potassium-rich wine stone and their application for high-performance removal. J Hazard Mater 2019;374:238–47. https://doi.org/10.1016/j.jhazmat.2019.04.042.

[19] Yaraş A, Arslanoğlu H. Efficient removal of basic yellow 51 dye via carbonized paper mill sludge using sulfuric acid. Sigma J Eng Nat Sci 2018;36(3):803–18.

[20] Arslanoğlu H, Kaya S, Tümen F. Cr (VI) adsorption on low-cost activated carbon developed from grape marc-vinasse mixture. Particul. Sci. Technol. 2019;38(6):768–81.

[21] Güler O, Gür F, Tümen F, Özer A. A study on the removal of heavy metals by carbonatisation cake discarded in sugar industry. Int Sugar J 2002;104:458–63.
[22] Magdy YH, Daifullah AAM. Adsorption of a basic dye from aqueous solutions onto sugar-industry-mud in two modes of operations. Waste Manag 1998;18(4):219–26. https://doi.org/10.1016/S0956-053X(98)00022-1.
[23] Vaccari G, Tamburini E, Sgualdino G, Urbaniec K, Klemeš J. Overview of the environmental problems in beet sugar processing: possible solutions. J Clean Prod 2005;13(5):499–507. https://doi.org/10.1016/j.jclepro.2003.09.008.
[24] APHA-AWWA/WEF. Standard methods for the examination of water and wastewater. 20th ed. Washington DC: American Public Health Association; 1998 [USA].
[25] Koroleva LF, Larionov LP, Gorbunova NP. Biomaterial based on doped calcium carbonate-phosphate for active osteogenesis. J. Biomater. Nanobiotechnol. 2012;3(2):226–37. https://doi.org/10.4236/jbnb.2012.32028.
[26] Schneider M, Günter C, Taubert A. Co-Deposition of a hydrogel/calcium phosphate hybrid layer on 3D printed poly (lactic acid) scaffolds via dip coating: towards automated biomaterials fabrication. Polym 2018;10(3):275. https://doi.org/10.3390/polym10030275.
[27] Reig FB, Adelantado JG, Moreno MM, Reig FB, Adelantado JG, Moreno MM. FTIR quantitative analysis of calcium carbonate (calcite) and silica (quartz) mixtures using the constant ratio method. Application to geological samples. Talanta 2002;58(4):811–21. https://doi.org/10.1016/S0039-9140(02)00372-7.
[28] Ha BJ, Park S. Classification of gallstones using Fourier-transform infrared spectroscopy and photography. Biomater Res 2018;22(1):18. https://doi.org/10.1186/s40824-018-0128-8.
[29] Wang S, Wu H. Environmental-benign utilisation of fly ash as low-cost adsorbents. J Hazard Mater 2006;136(3):482–501. https://doi.org/10.1016/j.jhazmat.2006.01.067.
[30] Koga N, Nakagoe YUZOU, Tanaka H. Crystallization of amorphous calcium carbonate. Thermochim Acta 1998;318(1–2):239–44. https://doi.org/10.1016/S0040-6031(98)00348-7.
[31] Souza DAD, Araujo DMD, Carvalho CDF, Yoshida MI. Physico-chemical analysis of flexible polyurethane foams containing commercial calcium carbonate. Mater Res 2008;11(4):433–8. https://doi.org/10.1590/S1516-14392008000400009.
[32] Tulyaganov DU, Agathopoulos S, Ventura JM, Karakassides MA, Fabrichnaya O, Ferreira JMF. Synthesis of glass–ceramics in the CaO–MgO–SiO2 system with B2O3, P2O5, Na2O and CaF2 additives. J Eur Ceram Soc 2006;26(8):1463–71. https://doi.org/10.1016/j.jeurceramsoc.2005.02.009.
[33] Cristiano E, Hu Y-J, Siegfried M, Kaplan D, Nitsche H. A comparison of point of zero charge measurement methodology. Clay Clay Miner 2011;59:107–15. https://doi.org/10.1346/CCMN.2011.0590201.
[34] Moulin P, Roques H. Zeta potential measurement of calcium carbonate. J Colloid Interface Sci 2003;261(1):115–26. https://doi.org/10.1016/S0021-9797(03)00057-2.
[35] Mondal NK, Bhaumik R, Datta JK. Fluoride adsorption by calcium carbonate, activated alumina and activated sugarcane ash. Environ Processes 2016;3(1):195–216. https://doi.org/10.1007/s40710-016-0130-x.
[36] Eren MŞ, Arslanoğlu H, Çiftçi H. Production of microporous Cu-doped BTC (Cu-BTC) metal-organic framework composite materials, superior adsorbents for the removal of methylene blue (Basic Blue 9). J Environ Chem Eng 2020;8(5):104247.
[37] Wu L, Forsling W, Schindler PW. Surface complexation of calcium minerals in aqueous solution: 1. Surface protonation at fluorapatite—water interfaces. J Colloid Interface Sci 1991;147(1):178–85. https://doi.org/10.1016/0021-9797(91)90145-X.
[38] Hartley AM, House WA, Callow ME, Leadbeater BSC. Coprecipitation of phosphate with calcite in the presence of photosynthesizing green algae. Water Res 1997;31(9):2261–8. https://doi.org/10.1016/S0043-1354(97)00103-6.
[39] Somasundaran P, Agar GE. The zero point of charge of calcite. J Colloid Interface Sci 1967;24(4):433–40. https://doi.org/10.1016/0021-9797(67)90241-X.
[40] Somasundaran P. Zeta potential of apatite in aqueous solutions and its change during equilibration. J Colloid Interface Sci 1968;27(4):659–66. https://doi.org/10.1016/0021-9797(68)90098-2.
[41] De Kanel J, Morse JW. The chemistry of orthophosphate uptake from seawater on to calcite and aragonite. Geochem Cosmochim Acta 1978;42(9):1335–40. https://doi.org/10.1016/0016-7037(78)90038-8.
[42] Thommes M, Kaneko K, Neimark AV, Olivier JP, Rodriguez-Reinoso F, Rouquerol J, et al. Physisorption of gases, with special reference to the evaluation of surface area and pore size distribution (IUPAC Technical Report). Pure Appl Chem 2015;87(9–10):1051–69.
[43] Yaraş A, Arslanoğlu H. Utilization of paper mill sludge for removal of cationic textile dyes from aqueous solutions. Sep Sci Technol 2019;54(16):2555–66.
[44] Chergui A, Bakhti M, Chahboub A, Haddoum S, Selatnia A, Junter Chergui G, et al. Simultaneous biosorption of Cu2+, Zn2+ and Cr6+ from aqueous solution by Streptomyces rimosus biomass. Desalin 2007;206(1–3):179–84. https://doi.org/10.1016/j.desal.2006.03.566.
[45] Anupam K, Dutta S, Bhattacharjee C, Datta S. Adsorptive removal of chromium (VI) from aqueous solution over powdered activated carbon: optimisation through response surface methodology. Chem Eng J 2011;173(1):135–43. https://doi.org/10.1016/j.cej.2011.07.049.
[46] Yaraş A, Arslanoğlu H. Valorization of paper mill sludge as adsorbent in adsorption process of copper (II) ion from synthetic solution: kinetic, isotherm and thermodynamic studies. Arabian J Sci Eng 2018;43(5):2393–402.
[47] Arslanoğlu H, Orhan R, Turan MD. Application of response surface methodology for the optimization of copper removal from aqueous solution by activated carbon prepared using waste polyurethane. Anal Lett 2019;53(9):1343–65.
[48] Lagergren S. Zur theorie der sogenannten adsorption geloster stoffe, Kungliga svenska vetenskapsakademiens. Handlingar 1898;24:1–39.
[49] Ho YS, McKay G. Pseudo-second order model for sorption processes. Process Biochem 1999;34:451–65. https://doi.org/10.1016/S0032-9592(98)00112-5.
[50] Weber WJ, Morris JC. Kinetics of adsorption on carbon from solution. J Sanit Eng Div 1963;89:31–60.
[51] Arslanoglu H. Adsorption of micronutrient metal ion onto struvite to prepare slow release multielement fertilizer: copper (II) doped-struvite. Chemosphere 2019;217:393–401. https://doi.org/10.1016/j.chemosphere.2018.10.207.
[52] Smith JM. Chemical reaction engineering. 3rd ed. New Delhi: McGraw Hill International Editions; 1981.
[53] Arslanoglu H, Altundogan HS, Tumen F. Preparation of cation exchanger from lemon and sorption of divalent heavy metals. Bioresour Technol 2008;99(7):2699–705.
[54] Arslanoglu H, Altundogan HS, Tumen F. Heavy metals binding properties of esterified lemon. J Hazard Mater 2009;164(2–3):1406–13. https://doi.org/10.1016/j.jhazmat.2008.09.054.

[55] Langmuir I. The adsorption of gases on plane surfaces of glass, mica and platinum. J Am Chem Soc 1918;40(9):1361–403.
[56] Herbert F. Über die adsorption in lösungen. Z Phys Chem 1907;57(1):385–470.
[57] Dubinin MM, Radushkevich LV. The equation of the characteristic curve of the activated charcoal. Proc Acad Sci Phys Chem Sect USSR 1947;55:331–7.
[58] Arslanoglu H. Removal of Cu (II) from aqueous solutions by using marble waste. Pamukkale Univ J Eng Sci 2017;23:877–86. https://doi.org/10.5505/pajes.2016.75688.
[59] Gordon M, Otterburn MS, Sweeney AG. Surface mass transfer processes during colour removal from effluent using silica. Water Res 1981;15:327–31.
[60] Boyd GE, Adamson AW, Myers JLS. The exchange adsorption of ions from aqueous solutions by organic zeolites. II. Kinetics. J Am Chem Soc 1947;69(11):2836–48.
[61] Naiya TK, Bhattacharya AK, Das SK. Adsorption of Cd (II) and Pb (II) from aqueous solutions on activated alumina. J Colloid Interface Sci 2009;333(1):14–26. https://doi.org/10.1016/j.jcis.2009.01.003.
[62] Lǔ J, Liu H, Liu R, Zhao X, Sun L, Qu J. Adsorptive removal of phosphate by a nanostructured Fe–Al–Mn trimetal oxide adsorbent. Powder Technol 2013;233:146–54. https://doi.org/10.1016/j.powtec.2012.08.024.
[63] Mdlalose L, Balogun M, Setshedi K, Chimuka L, Chetty A. Adsorption of phosphates using transition metals-modified bentonite clay. Sep Sci Technol 2018:1–12. https://doi.org/10.1080/01496395.2018.1547315.
[64] Li R, Wang JJ, Zhou B, Awasthi MK, Ali A, Zhang Z, et al. Enhancing phosphate adsorption by Mg/Al layered double hydroxide functionalized biochar with different Mg/Al ratios. Sci Total Environ 2016;559:121–9. https://doi.org/10.1016/j.scitotenv.2016.03.151.
[65] Ren Z, Shao L, Zhang G. Adsorption of phosphate from aqueous solution using an iron–zirconium binary oxide sorbent. Water Air Soil Pollut 2012;223(7):4221–31. https://doi.org/10.1007/s11270-012-1186-5.
[66] Özacar M. Equilibrium and kinetic modelling of adsorption of phosphorus on calcined alunite. Adsorpt 2009;9:125–32.
[67] Zhang M, Bin G. Removal of arsenic, methylene blue, and phosphate by biochar/AlOOH nanocomposite. Chem Eng J 2013;226:286–92. https://doi.org/10.1016/j.cej.2013.04.077.
[68] Mangwandi C, Albadarin AB, Glocheux Y, Walker GM. Removal of ortho-phosphate from aqueous solution by adsorption onto dolomite. J Environ Chem Eng 2014;2(2):1123–30. https://doi.org/10.1016/j.jece.2014.04.010.